

# Skyrmion spacetime defect

F.R. Klinkhamer\*

*Institute for Theoretical Physics,  
Karlsruhe Institute of Technology (KIT),  
76128 Karlsruhe, Germany*

## Abstract

A finite-energy static classical solution is obtained for standard Einstein gravity coupled to an  $SO(3) \times SO(3)$  chiral model of scalars [Skyrme model]. This nonsingular localized solution has nontrivial topology for both the spacetime manifold and the  $SO(3)$  matter fields. The solution corresponds to a single spacetime defect embedded in flat Minkowski spacetime.

PACS numbers: 04.20.Cv, 02.40.Pc

Keywords: general relativity, topology

---

\* frans.klinkhamer@kit.edu

## I. INTRODUCTION

The classical spacetime emerging from a quantum-spacetime phase may very well have nontrivial structure at small length scales [1–3]. This nontrivial structure affects, in particular, the propagation of electromagnetic waves [4]. The question remains as to what the small-scale structure embedded in a flat spacetime really looks like (here, we do not consider intra-universe wormhole solutions which connect *two* asymptotically flat spaces [3]).

Narrowing down the question, is it possible at all to have nonsingular localized finite-energy solutions of the standard Einstein equations with an asymptotically flat spacetime? For one particular topology studied in Ref. [4], it has been suggested [5] to consider an  $SO(3)$  Skyrme model coupled to gravity [6–11].

For this specific theory and topology, two nonsingular defect solutions have been found recently, a vacuum solution and a nonvacuum solution [12]. (Corresponding nonsingular black-hole solutions were presented in Refs. [13, 14].) Both defect solutions of Ref. [12] are localized, but the one with a nonvanishing scalar  $SO(3)$  field has infinite energy and trivial topology (i.e., zero winding number or “baryon” number). It has been conjectured that this particular non-vacuum solution is unstable and decays to a Skymion-like defect solution (with unit winding number or “baryon” charge) by emitting out-going waves of scalars. Such a nonsingular Skymion defect solution is constructed in the present article.

## II. THEORY

The setup of the theory has been described elsewhere in detail [12–15], but, for completeness, we recall the main steps.

### A. Manifold

The 4-dimensional spacetime manifold considered in this article has the topology

$$M_4 = \mathbb{R} \times M_3. \tag{1a}$$

The 3-space  $M_3$  carries the nontrivial topology and is, in fact, a noncompact, orientable, nonsimply-connected manifold without boundary. Up to a point,  $M_3$  is homeomorphic to the 3-dimensional real-projective space,

$$M_3 \simeq \mathbb{R}P^3 - \{\text{point}\}. \tag{1b}$$

Adding the “point at infinity,” gives the compact space  $\overline{M}_3 \simeq \mathbb{R}P^3$ .

For the direct construction of  $M_3$ , we perform local surgery on the 3-dimensional Euclidean space  $E_3 = (\mathbb{R}^3, \delta_{mn})$ . Recall the standard Cartesian and spherical coordinates on  $\mathbb{R}^3$ ,

$$\vec{x} \equiv |\vec{x}| \hat{x} = (x^1, x^2, x^3) = (r \sin \theta \cos \phi, r \sin \theta \sin \phi, r \cos \theta), \quad (2)$$

with  $x^m \in (-\infty, +\infty)$ ,  $r \geq 0$ ,  $\theta \in [0, \pi]$ , and  $\phi \in [0, 2\pi)$ . Now, we obtain  $M_3$  from  $\mathbb{R}^3$  by removing the interior of the ball  $B_b$  with radius  $b$  and identifying antipodal points on the boundary  $S_b \equiv \partial B_b$ . Denoting point reflection by  $P(\vec{x}) = -\vec{x}$ , the 3-space  $M_3$  is given by

$$M_3 = \{ \vec{x} \in \mathbb{R}^3 : (|\vec{x}| \geq b > 0) \wedge (P(\vec{x}) \cong \vec{x} \text{ for } |\vec{x}| = b) \}, \quad (3)$$

where  $\cong$  stands for point-wise identification (Fig. 1). A minimal noncontractible loop (with length  $\pi b$  in  $E_3$ ) corresponds to half of a great circle on the  $r = b$  sphere in  $E_3$ , taken between antipodal points which are to be identified.

The single set of coordinates (2) does not suffice for an appropriate description of  $M_3$ . The reason is that two different values of these coordinates may correspond to one point of  $M_3$ . An example is given by the two sets of coordinates  $\vec{x} = (0, b, 0)$  and  $\vec{x} = (0, -b, 0)$ , which describe the same point of  $M_3$ .

A particular covering of  $M_3$  uses three charts of coordinates, labeled by  $n = 1, 2, 3$ . The basic idea [5] is that the coordinates resemble spherical coordinates and that each coordinate chart surrounds one of the three Cartesian coordinate axes. These coordinates are denoted

$$(X_n, Y_n, Z_n), \quad \text{for } n = 1, 2, 3. \quad (4)$$

In each chart, there is one polar-type angular coordinate of finite range, one azimuthal-type angular coordinate of finite range, and one radial-type coordinate with infinite range. Specifically, the coordinates have the following ranges:

$$X_1 \in (-\infty, \infty), \quad Y_1 \in (0, \pi), \quad Z_1 \in (0, \pi), \quad (5a)$$

$$X_2 \in (0, \pi), \quad Y_2 \in (-\infty, \infty), \quad Z_2 \in (0, \pi), \quad (5b)$$

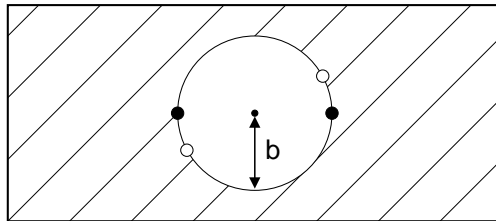


Figure 1. Three-space  $M_3$  obtained by surgery on  $\mathbb{R}^3$ : interior of the ball with radius  $b$  removed and antipodal points on the boundary of the ball identified (as indicated by open and filled circles).

$$X_3 \in (0, \pi), \quad Y_3 \in (0, \pi), \quad Z_3 \in (-\infty, \infty). \quad (5c)$$

The different charts overlap in certain regions: see Appendix B of Ref. [14] for further details.

## B. Fields and interactions

The spacetime manifold (1) of the previous section is now supplemented with a metric  $g_{\mu\nu}(X)$ , whose dynamics is taken to be governed by the standard Einstein–Hilbert action. In addition, we consider a scalar field  $\Omega(X) \in SO(3)$  with self-interactions governed by a quartic Skyrme term in the action [6, 7].

The combined action of the pure-gravity sector and the matter sector is given by ( $c = \hbar = 1$ )

$$S = \int_{M_4} d^4X \sqrt{-g} \left[ \frac{1}{16\pi G_N} R + \frac{f^2}{4} \text{tr}(\omega_\mu \omega^\mu) + \frac{1}{16e^2} \text{tr}([\omega_\mu, \omega_\nu][\omega^\mu, \omega^\nu]) \right], \quad (6)$$

in terms of the Ricci curvature scalar  $R$  and the definition  $\omega_\mu \equiv \Omega^{-1} \partial_\mu \Omega$ . The kinetic term of the scalar field involves the mass scale  $f$ . The Skyrme term corresponds to the trace of the square of the commutator  $[\omega_\mu, \omega_\nu]$  and has dimensionless coupling constant  $1/e^2$ .

The  $SO(3) \times SO(3)$  global symmetry of the matter sector is realized on the scalar field by the following transformation with constant parameters  $S_L, S_R \in SO(3)$ :

$$\Omega(X) \rightarrow S_L \cdot \Omega(X) \cdot S_R^{-1}, \quad (7)$$

where the central dot denotes matrix multiplication. The generic argument  $X$  of the fields and the measure  $d^4X$  in the integral (6) correspond to one of the three different coordinate charts needed to cover  $M_4$ .

## C. Ansatz

A spherically symmetric *Ansatz* for the metric is given by the following line element:

$$ds^2 \Big|_{\text{chart-2}} = -[\tilde{\mu}(W)]^2 dT^2 + (1 - b^2/W) [\tilde{\sigma}(W)]^2 (dY_2)^2 + W \left[ (dZ_2)^2 + \sin^2 Z_2 (dX_2)^2 \right], \quad (8a)$$

$$W \Big|_{\text{chart-2}} \equiv b^2 + (Y_2)^2, \quad (8b)$$

and similarly for the chart-1 and chart-3 domains [14, 15]. The focus on chart-2 coordinates in (8) is purely for cosmetic reasons.

The scalar field is described by a Skyrmion-type *Ansatz* [5–7],

$$\Omega = \cos [\tilde{F}(r^2)] \mathbb{1}_3 - \sin [\tilde{F}(r^2)] \hat{x} \cdot \vec{S} + (1 - \cos [\tilde{F}(r^2)]) \hat{x} \otimes \hat{x}, \quad (9a)$$

$$\tilde{F}(b^2) = \pi, \quad (9b)$$

$$S_1 \equiv \begin{pmatrix} 0 & 0 & 0 \\ 0 & 0 & 1 \\ 0 & -1 & 0 \end{pmatrix}, \quad S_2 \equiv \begin{pmatrix} 0 & 0 & -1 \\ 0 & 0 & 0 \\ 1 & 0 & 0 \end{pmatrix}, \quad S_3 \equiv \begin{pmatrix} 0 & 1 & 0 \\ -1 & 0 & 0 \\ 0 & 0 & 0 \end{pmatrix}, \quad (9c)$$

with a hedgehog term proportional to  $\sin \tilde{F}$  and further terms involving the  $3 \times 3$  unit matrix  $\mathbb{1}_3$  and another matrix which reads in components  $(\hat{x} \otimes \hat{x})^{ab} = \hat{x}^a \hat{x}^b$ . The boundary condition (9b) at  $r \equiv |\vec{x}| = b$  makes it possible to employ the single coordinate chart (2). This observation relies on the following equality:

$$\Omega(r, \hat{x})|_{r=b} = -\mathbb{1}_3 + 2\hat{x} \otimes \hat{x} = \Omega(r, -\hat{x})|_{r=b}, \quad (10)$$

which gives the same scalar field  $\Omega$  for antipodal points on the  $r = b$  sphere in  $\mathbb{R}^3$ , allowing these antipodal points to be identified in order to obtain  $M_3$ . In order to match the coordinates used for the metric (8), we make the identification  $r^2 = b^2 + Y_2^2$  and the explicit relations between  $\hat{x}$  and  $(X_2, Z_2)$  can be found in Refs. [14, 15].

An alternative *Ansatz* based on Painlevé–Gullstrand-type coordinates [16–18] is presented in Appendix A.

#### D. Reduced field equations

At this moment, we introduce the following dimensionless model parameters and dimensionless variables:

$$\tilde{\eta} \equiv 8\pi\eta \equiv 8\pi G_N f^2, \quad (11a)$$

$$w \equiv (ef)^2 W = (y_0)^2 + y^2, \quad (11b)$$

$$y \equiv ef Y_2, \quad (11c)$$

$$y_0 \equiv ef b. \quad (11d)$$

Inserting the *Ansatz* of Sec. II C into the Einstein and matter field equations from the action (6) gives the corresponding reduced expressions [5, 8, 12]. From these equations written in terms of the dimensionless variables (11), we obtain the following three ordinary differential

equations (ODEs):

$$\begin{aligned}\tilde{\sigma}'(w) = & \tilde{\sigma}(w) \left( - \left[ w - 2\tilde{\eta} \left( 1 + 2w - \cos[\tilde{F}(w)] \right) \sin^2[\tilde{F}(w)/2] \right] \tilde{\sigma}(w)^2 \right. \\ & + w \left[ 1 + 2\tilde{\eta} \left( 2w^3(1 + y_0^2) - 2y_0^2(1 + y_0^2)(y_0^4 - 1) + 2w y_0^2(3y_0^2 + 3y_0^4 - 1) \right. \right. \\ & \left. \left. - w^2(6y_0^2 + 6y_0^4 - 1) - 2w \cos[\tilde{F}(w)] \right) \tilde{F}'(w)^2 \right] \right) / (4w^2),\end{aligned}\quad (12a)$$

$$\begin{aligned}\tilde{\mu}'(w) = & \tilde{\mu}(w) \left( \left[ w - 2\tilde{\eta} \left( 1 + 2w - \cos[\tilde{F}(w)] \right) \sin^2[\tilde{F}(w)/2] \right] \tilde{\sigma}(w)^2 \right. \\ & \left. + w \left[ -1 + 2w\tilde{\eta} \left( 2 + w - 2\cos[\tilde{F}(w)] \right) \tilde{F}'(w)^2 \right] \right) / (4w^2),\end{aligned}\quad (12b)$$

$$\begin{aligned}\tilde{F}''(w) = & \left( \left[ 3 \left( 1 + w - \cos[\tilde{F}(w)] \right) \sin[\tilde{F}(w)] - \left( 2 + w - 2\cos[\tilde{F}(w)] \right) \right. \right. \\ & \times \left( 3w - 2\tilde{\eta}(3 + 6w - 3\cos[\tilde{F}(w)]) \sin^2[\tilde{F}(w)/2] \right) \tilde{F}'(w) \left. \right] \tilde{\sigma}(w)^2 \\ & \left. - 6w^2 \left[ 1 + \sin[\tilde{F}(w)] \tilde{F}'(w) \right] \tilde{F}'(w) \right) / \left( 2w^2 \left[ 6 + 3w - 6\cos[\tilde{F}(w)] \right] \right),\end{aligned}\quad (12c)$$

where the prime stands for differentiation with respect to  $w$ .

The ODEs (12) are to be solved with the following boundary conditions:

$$\tilde{F}(y_0^2) = \pi, \quad \tilde{F}(\infty) = 0, \quad (13a)$$

$$\tilde{\sigma}(\infty) = 1, \quad \tilde{\mu}(\infty) = 1. \quad (13b)$$

The three boundary conditions at infinity provide for asymptotic flatness and the boundary condition  $\tilde{F} = \pi$  at the core gives a topologically nontrivial scalar field configuration, that is, a Skyrmin-like configuration with winding number unity. In fact, the winding number or topological degree of the compactified map  $\Omega : \overline{M}_3 \rightarrow SO(3)$  turns out to be given by [5, 7]

$$\deg[\Omega] = \frac{2}{\pi} \int_0^\pi d\tilde{F} \sin^2(\tilde{F}/2) = 1, \quad (14)$$

where the endpoints of the integral on the right-hand side correspond to boundary conditions (13a).

### III. NUMERICAL SOLUTION

In order to obtain the numerical solution corresponding to the *Ansatz* from Sec. II C, we have adopted the following procedure. The boundary condition on the three functions  $\tilde{F}(w)$ ,  $\tilde{\sigma}(w)$ , and  $\tilde{\mu}(w)$  are set at the defect core  $w = y_0^2$ . Specifically, we take

$$\tilde{F}(y_0^2) = \pi, \quad \tilde{F}'(y_0^2) = \alpha, \quad (15a)$$

$$\tilde{\sigma}(y_0^2) = \beta, \quad \tilde{\mu}(y_0^2) = \gamma, \quad (15b)$$

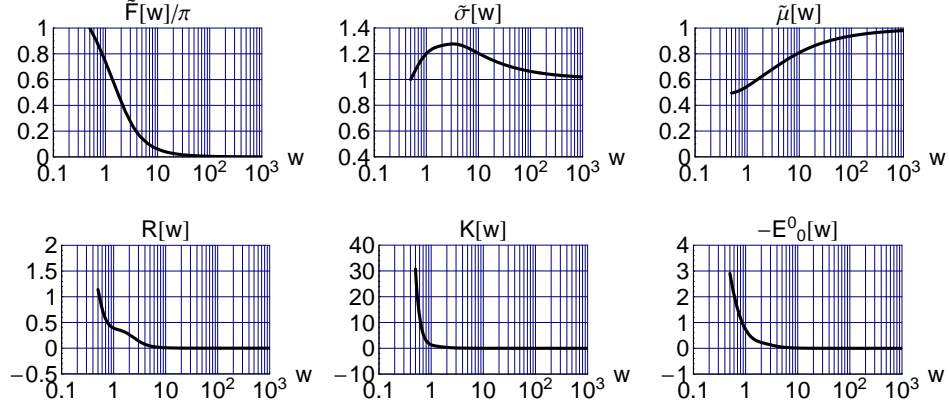


Figure 2. Top row: functions  $\tilde{F}(w)$ ,  $\tilde{\sigma}(w)$ , and  $\tilde{\mu}(w)$  of the numerical solution of the reduced field equations (12). The model parameters are  $y_0 = 1/\sqrt{2}$  and  $\tilde{\eta} = 1/20$ . The boundary conditions at the defect core  $w = y_0^2 = 1/2$  are:  $\tilde{F} = \pi$ ,  $\tilde{F}' = -1.9454$ ,  $\tilde{\sigma} = 1.0000$ , and  $\tilde{\mu} = 0.494872$ . Bottom row: corresponding dimensionless Ricci scalar  $R$ , dimensionless Kretschmann scalar  $K$ , and the negative of the 00-component of the dimensionless Einstein tensor  $E^\mu_\nu$ ; see Appendix B for details.

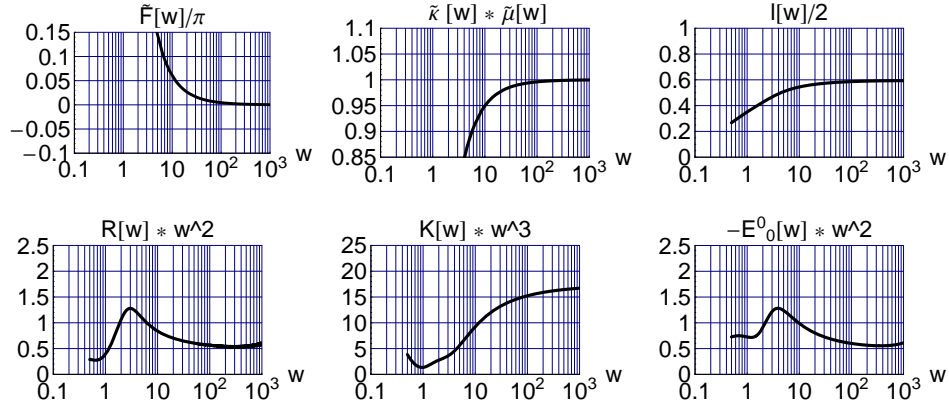


Figure 3. Asymptotic behavior of the functions from Fig. 2, with definitions  $\tilde{\kappa}(w) \equiv \sqrt{1 - y_0^2/w} \tilde{\sigma}(w)$  and  $l(w) \equiv [1 - \tilde{\mu}(w)^2] \sqrt{w}$ .

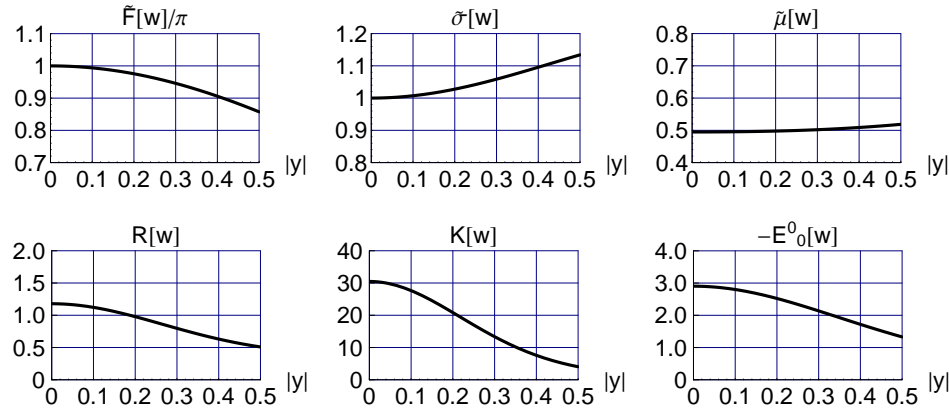


Figure 4. Core behavior of the functions from Fig. 2, plotted with respect to the dimensionless quasi-radial coordinate  $y \in \mathbb{R}$  of the chart-2 domain. The coordinate  $w$  is given by  $w = y_0^2 + y^2$ .

for certain initial values  $\alpha, \beta, \gamma \in \mathbb{R}$ . With these boundary conditions, the ODEs (12) are solved over  $w \in [y_0^2, w_{\max}]$  for sufficiently large values of  $w_{\max}$ . Next, the numbers  $\alpha$  and  $\beta$  in (15) are varied in order to obtain vanishing  $F(w)$  and  $F'(w)$  at  $w = w_{\max}$ . The obtained function  $\tilde{\mu}(w)$  can then be re-scaled in order to obtain at  $w = w_{\max}$  the Schwarzschild-type values

$$\tilde{\mu}(w_{\max}) = (1 - \bar{l}(w_{\max})/\sqrt{w_{\max}}), \quad (16a)$$

$$\tilde{\sigma}(w_{\max}) = 1/(1 - \bar{l}(w_{\max})/\sqrt{w_{\max}}), \quad (16b)$$

with a dimensionless length parameter  $\bar{l}(w_{\max})$ .

Numerical results for the dimensionless gravitational coupling constant  $\tilde{\eta} = 1/20$  and the dimensionless defect size  $y_0 = 1/\sqrt{2}$  are given in Figs. 2–4. Several comments are in order. First, the results from the bottom row panels in Fig. 2 make clear that the solution is localized. Second, the middle and right panels of the top row in Fig. 3 show the Schwarzschild behavior (16) for  $w \gtrsim 100$ . Third, it appears that the energy-density  $T_0^0 = E_0^0/\tilde{\eta}$  from the bottom right panel of Fig. 3 behaves asymptotically as  $1/w^2 \sim 1/|y|^4$ , which results in a finite integral. Fourth, the physical quantities shown in the bottom row of Fig. 4 behave smoothly at the defect core ( $Y_2 = 0$ ) and the Ricci scalar, for example, is nonsingular there.

Similar results have been obtained for other values of the dimensionless defect size  $y_0$ , provided they are not too small:  $y_0 > y_{0,\text{crit}}$  with  $y_{0,\text{crit}} \sim 1/(2\sqrt{2})$  for coupling constant  $\tilde{\eta} = 1/20$ . Table I gives the corresponding values for the dimensionless Schwarzschild mass  $\hat{m}$ .

Table I. Numerical results for the dimensionless Schwarzschild mass  $\hat{m} \equiv 4\pi l/\tilde{\eta}$  in the theory with dimensionless gravitational coupling constant  $\tilde{\eta} = 1/20$ . The dimensionless length parameter  $l$  is obtained from the numerical solution by use of (16a). Also shown are the values of the flat-spacetime energy integral  $E^{\text{flat}}$  relative to its Bogomolnyi value  $12\sqrt{2}\pi^2 f/e$ . This integral  $E^{\text{flat}}$  depends only on the Skyrme function  $\tilde{F}(w)$  and has both metric functions  $\tilde{\sigma}(w)$  and  $\tilde{\mu}(w)$  set to unity; see Appendix B. As such,  $E^{\text{flat}}[\tilde{F}]$  can be used as a diagnostic of the Skyrme function  $\tilde{F}(w)$ .

$y_0$	$l/2$	$\hat{m}$	$E^{\text{flat}}/E_{\text{Bogomolnyi}}^{\text{flat}}$
$1/(2\sqrt{2})$	—	—	—
$1/2$	0.389	97.8	1.36
$1/\sqrt{2}$	0.593	149	1.28
1	0.919	231	1.35
$\sqrt{2}$	1.33	333	1.60



Qualitatively, these  $\widehat{m}$  values agree with those of Fig. 8.7b in Ref. [5], but not quantitatively. This quantitative difference, most likely, traces back to the fact that the fields of Ref. [5] do not solve the Einstein equations at the defect core proper,  $W = b^2$  in our notation. This then results in a different behavior of the fields further out,  $W > b^2$ , making for different numerical values of  $\widehat{m}$ .

The present paper presents only exploratory numerical results, with the sole purpose of establishing the existence of at least one class of Skyrmion-like spacetime-defect solutions. More numerical work is clearly needed. For example, it remains to be seen if our nonsingular defect would have another branch of solutions (cf. Fig. 8.7a in Ref. [5]) where  $\widehat{m}(y_0)$  would have a genuine minimum for an intermediate value of  $y_0$ , similar to that of the flat-spacetime non-gravitating solution with energy  $E^{\text{flat}}(y_0)$ ; see the caption of Table I for further discussion and Appendix B for the definition of the integral.

#### IV. DISCUSSION

In this article, we have succeeded in constructing a nonsingular localized finite-energy solution of the standard Einstein equations with an asymptotically flat spacetime. The particular topology is given in (1) and the matter content by a Skyrme model with action (6). The three crucial inputs for obtaining the solution are, first, a proper set of coordinates (Sec. II A), second, an appropriate *Ansatz* (Sec. II C), and, third, special attention to the behavior of the fields at the defect core for the numerical solution (Sec. III).

It remains to be proven that the obtained solution is stable, but we are moderately optimistic. This optimism is based on the fact that the scalar fields by themselves would be stable because of the topological charge (14). Still, a rigorous proof for the stability of the self-gravitating solution would be most welcome. (Equally welcome would be a rigorous proof for the *existence* of the self-gravitating solution, as we have relied on a numerical solution of the reduced field equations.)

In Refs. [13, 14], we have given a heuristic discussion how the corresponding nonsingular black-hole solutions could appear in physical situations of spherical gravitational collapse in an essentially flat spacetime with trivial topology. The scenario is that, when the central matter density becomes large enough, there is a quantum jump [1, 2] from the trivial  $\mathbb{R}^4$  topology to the nonsimply-connected  $M_4$  topology of the nonsingular solution, with a noncontractible-loop length scale  $b$  of the order of the quantum-gravity length scale  $L_{\text{Planck}} \equiv (\hbar G_N/c^3)^{1/2}$ . (Perhaps topology change is not needed if the nontrivial small-scale topology is already present as a remnant from a quantum spacetime foam [15].)

If a similar discussion applies to the case of the Skyrmion spacetime defect found in this paper, it can be conjectured that defects with the smallest possible value of the mass

$\widehat{M}$  would have the largest probability of occurring. For the branch of classical solutions shown in Table I, this would imply a preferred value of the defect size of approximately  $b \equiv y_0/(ef) \sim 0.5/(ef)$  for a mass of approximately  $\widehat{M} \equiv \widehat{m} f/e \sim 100 f/e$ .

At this moment, we should mention that the metric (8) of the nonsingular defect solution does have a minor blemish [13, 15]: at  $W = b^2$ , it cannot be brought to a patch of Minkowski spacetime by a genuine diffeomorphism (a  $C^\infty$  function) but only by a  $C^1$  function. This may very well be the price to pay for having a nonsingular solution. The ultimate quantum theory of spacetime and gravity will determine which role (if any) these nonsingular defect-type classical solutions play for the origin of classical spacetime in the very early universe.

## ACKNOWLEDGMENTS

It is a pleasure to thank C. Rahmede for discussions.

## Appendix A: Alternative Ansatz

In this appendix, we present an alternative *Ansatz*, possibly relevant for nonsingular black-hole solutions with topology (1) and defect size  $b$ .

The new form of the *Ansatz* is related to the one of (8) by the introduction of a new time coordinate,  $\widehat{T} = \widehat{T}(T, Y_2)$ . This new coordinate follows from considering freely-moving observers falling in along radial geodesics and writing their covariant 4-velocities as gradients of a new time function  $\widehat{T}$ . As such, the procedure is analogous to that of changing the standard coordinates of the Schwarzschild metric to the Painlevé–Gullstrand coordinates [16–18], generalized to other static spherically symmetric spacetimes (cf. Sec. IV of Ref. [18]).

In this way, we arrive at the following *Ansatz* for the line element:

$$ds^2 \Big|_{\text{chart-2}} = -d\widehat{T}^2 + \left[ \widetilde{\chi}(W) \frac{Y_2}{\sqrt{W}} dY_2 + \widetilde{\xi}(W) d\widehat{T} \right]^2 + W \left[ (dZ_2)^2 + \sin^2 Z_2 (dX_2)^2 \right], \quad (\text{A1a})$$

$$W \Big|_{\text{chart-2}} \equiv b^2 + (Y_2)^2, \quad (\text{A1b})$$

with functions  $\widetilde{\chi}(W)$  and  $\widetilde{\xi}(W)$ . A similar *Ansatz* holds for the chart-1 and chart-3 domains; see Appendix C of Ref. [15]. The *Ansatz* for the scalar  $SO(3)$  field remains as given in Sec. II C. The boundary conditions are given by (13a) for the Skyrme function and by  $\widetilde{\chi}(\infty) = 1$  and  $\widetilde{\xi}(\infty) = 0$  for the new metric functions.

## Appendix B: Reduced expressions

In this appendix, we give the reduced expressions for certain curvature tensors. In addition, we give the expression for the flat-spacetime energy integral used in the table.

Specifically, consider the Ricci scalar  $R \equiv g^{\mu\nu} R_{\mu\nu}$ , the Kretschmann scalar  $K \equiv R_{\mu\nu\rho\sigma} R^{\mu\nu\rho\sigma}$ , and the 00-component of the Einstein tensor  $E^\mu{}_\nu \equiv R^\mu{}_\nu - (1/2) R \delta^\mu{}_\nu$ . Then, the *Ansatz* from Sec. II C produces the following expressions:

$$R(w) = 2(e f)^2 \left( \tilde{\mu}(w) \tilde{\sigma}(w)^3 - \tilde{\mu}(w) \tilde{\sigma}(w) - 6 w \tilde{\sigma}(w) \tilde{\mu}'(w) + 4 w \tilde{\mu}(w) \tilde{\sigma}'(w) + 4 w^2 \tilde{\mu}'(w) \tilde{\sigma}'(w) - 4 w^2 \tilde{\sigma}(w) \tilde{\mu}''(w) \right) / \left( w \tilde{\mu}(w) \tilde{\sigma}(w)^3 \right), \quad (\text{B1a})$$

$$K(w) = 4(e f)^4 \left( \tilde{\mu}(w)^2 \tilde{\sigma}(w)^2 - 2 \tilde{\mu}(w)^2 \tilde{\sigma}(w)^4 + \tilde{\mu}(w)^2 \tilde{\sigma}(w)^6 + 12 w^2 \tilde{\sigma}(w)^2 \tilde{\mu}'(w)^2 - 16 w^3 \tilde{\sigma}(w) \tilde{\mu}'(w)^2 \tilde{\sigma}'(w) + 8 w^2 \tilde{\mu}(w)^2 \tilde{\sigma}'(w)^2 + 16 w^4 \tilde{\mu}'(w)^2 \tilde{\sigma}'(w)^2 + 16 w^3 \tilde{\sigma}(w)^2 \tilde{\mu}'(w) \tilde{\mu}''(w) - 32 w^4 \tilde{\sigma}(w) \tilde{\mu}'(w) \tilde{\sigma}'(w) \tilde{\mu}''(w) + 16 w^4 \tilde{\sigma}(w)^2 \tilde{\mu}''(w)^2 \right) / \left( w^2 \tilde{\mu}(w)^2 \tilde{\sigma}(w)^6 \right), \quad (\text{B1b})$$

$$E^0{}_0(w) = (e f)^2 \left( \tilde{\sigma}(w) - \tilde{\sigma}(w)^3 - 4 w \tilde{\sigma}'(w) \right) / \left( w \tilde{\sigma}(w)^3 \right). \quad (\text{B1c})$$

We have set  $(e f) = 1$  for the results shown in Figs. 2–4.

Evaluating the negative of the matter Lagrange density from (6) with the *Ansatz* fields and setting the *Ansatz* metric functions  $\tilde{\sigma}(w)$  and  $\tilde{\mu}(w)$  to unity gives the flat-spacetime energy integral  $E^{\text{flat}}$  used in Table I:

$$E^{\text{flat}} = 4\pi (f/e) \int_{y_0^2}^{\infty} dw w^{-3/2} \left[ \left( 1 + \cos[\tilde{F}(w)] + 2w \right) \sin^2[\tilde{F}(w)/2] + w^2 \left( 2 - 2 \cos[\tilde{F}(w)] + w \right) \tilde{F}'(w)^2 \right], \quad (\text{B2})$$

which agrees with previous results [5–7].

- 
- [1] J.A. Wheeler, “On the nature of quantum geometrodynamics,” *Ann. Phys. (N.Y.)* **2**, 604 (1957).
  - [2] J.A. Wheeler, “Superspace and the nature of quantum geometrodynamics,” in: *Battelle Rencontres 1967*, edited by C.M. DeWitt and J.A. Wheeler (Benjamin, New York, 1968), Chap. 9.
  - [3] M. Visser, *Lorentzian Wormholes: From Einstein to Hawking* (Springer, New York, 1995).
  - [4] S. Bernadotte and F.R. Klinkhamer, “Bounds on length scales of classical spacetime foam models,” *Phys. Rev. D* **75**, 024028 (2007); arXiv:hep-ph/0610216.
  - [5] M. Schwarz, “Nontrivial spacetime topology, modified dispersion relations, and an  $SO(3)$ -Skyrme model,” PhD Thesis, KIT, July 9, 2010 (Verlag Dr. Hut, München, Germany, 2010).
  - [6] T.H.R. Skyrme, “A nonlinear field theory,” *Proc. Roy. Soc. Lond. A* **260**, 127 (1961).
  - [7] N.S. Manton and P. Sutcliffe, *Topological Solitons* (Cambridge Univ. Press, Cambridge, UK, 2004).
  - [8] N.K. Glendenning, T. Kodama, and F.R. Klinkhamer, “Skyrme topological soliton coupled to gravity,” *Phys. Rev. D* **38**, 3226 (1988).
  - [9] P. Bizon and T. Chmaj, “Gravitating skyrmions,” *Phys. Lett. B* **297**, 55 (1992).
  - [10] M. Heusler, N. Straumann, and Z.-H. Zhou, “Selfgravitating solutions of the Skyrme model and their stability,” *Helv. Phys. Acta* **66**, 614 (1993).
  - [11] B. Kleihaus, J. Kunz, and A. Sood, “ $SU(3)$  Einstein–Skyrme solitons and black holes,” *Phys. Lett. B* **352**, 247 (1995), arXiv:hep-th/9503087.
  - [12] F.R. Klinkhamer and C. Rahmede, “Nonsingular spacetime defect,” arXiv: 1303.7219.
  - [13] F.R. Klinkhamer, “Black-hole solution without curvature singularity,” *Mod. Phys. Lett. A* **28**, 1350136 (2013), arXiv:1304.2305.
  - [14] F.R. Klinkhamer, “Black-hole solution without curvature singularity and closed timelike curves,” *Acta Phys. Pol. B* **45**, 5 (2014), arXiv:1305.2875.
  - [15] F.R. Klinkhamer, “A new type of nonsingular black-hole solution in general relativity,” arXiv:1309.7011.
  - [16] P. Painlevé, “La mécanique classique et la théorie de la relativité,” *C. R. Acad. Sci. (Paris)* **173**, 677 (1921).
  - [17] A. Gullstrand, “Allgemeine Lösung des statischen Einkörper-problems in der Einsteinschen Gravitationstheorie,” *Arkiv. Mat. Astron. Fys.* **16**, 1 (1922).
  - [18] K. Martel and E. Poisson, “Regular coordinate systems for Schwarzschild and other spherical space-times,” *Am. J. Phys.* **69**, 476 (2001), arXiv:gr-qc/0001069.